Received: January 4, 2022. Revised: February 7, 2022.

INASS

International Journal of
Intelligent Engineering & Systems

http://www.inass.org/

Design of an Optimally Tuned Fractionalized PID Controller for DC Motor Speed Control Via a Henry Gas Solubility Optimization Algorithm

Abdelhakim Idir[1*] Khatir Khettab[1] Yassine Bensafia[2]

[1] *Department of Electrical Engineering, University Mohamed Boudiaf of M'sila, 28000, Algeria*
Applied Automation Laboratory, F.H.C., University of Boumerdes,
1 Av. de l'Independance, 35000 Boumerdes, Algeria
[2] *Department of Electrical Engineering, Bouira University, 10000, Algeria*
* Corresponding author's Email: abdelhakim.idir@univ-msila.dz

Abstract: The goal of this research is to develop a high-performance fractionalized proportional–integral–derivative (FPID) controller based on Henry Gas Solubility Optimization (HGSO) for controlling the speed of a direct current (DC) motor. The suggested HGSOA-based Fractionalized PID technique with Matsuda approximation method was used to obtain the optimal FPID controller by minimising the integral of time multiplied absolute error (ITAE) as the objective function. Index of performance and disturbance rejection analyses, as well as transient and frequency responses, were all employed to validate the suggested approach's effectiveness. The proposed HGSO-FPID controller with Matsuda approximation was then compared not only to the original HGSO algorithm-tuned PID controller, but also to other controllers tuned by cutting-edge meta-heuristic algorithms such as Atom Search Optimization algorithm (ASO), Grey Wolf Optimization algorithm (GWO), Particle Swarm Optimisation (PSO), Invasive Weed Optimisation (IWO), and stochastic fractal search (SFS). The results showed that the proposed HGSOA-FPID controller has better performance with lower settling time, Ts which 0.1003 s, with lower rise time, Tr which is 0.0579 s, negligible overshoot, D which is 0.0052% and strong output disturbance rejection when compared to the performance of the other controllers.

Keywords: Fractionalized PID (FPID), DC motor, HGSO algorithm, Optimal control, Approximation method.

1. Introduction

DC motors are widely employed in various industrial applications that demand a wide speed range. The advantage of dc motors may be the ability to control the speed. The word "speed control" refers to the purposeful change of speed, which can be done both automatically and manually. Different controllers are used to control the speed of DC motors; the most commonly used controllers are conventional controllers PI and PID [1, 2].

PID controllers, on the other hand, have some drawbacks, such as unwanted speed overshoot and sluggish response due to rapid changes in load torque, as well as sensitivity to controller gains K_i and K_P. The accuracy of system models and parameters determines the controller's performance. As a result, a controller that can overcome the drawbacks of PID controllers is required.

Proportional integral (PI), PID fuzzy logic controller (FLC), or a mix of the two: fuzzy-genetic algorithm, particle swarm optimization are examples of traditional and numeric controller types. One of the most prevalent methodologies in various industries is the proportional–integral–derivative (PID) design with a meta-heuristic algorithm. These later have recently become popular in optimization issues. Several algorithms have been created. Hashim et al. [3] highlighted one of the newest of them, Henry Gas Solubility Optimization (HGSO). Henry's law of physics influenced this algorithm. This algorithm has also been used in other papers [4-6]. For example, in [7] the authors conduct a performance comparison of

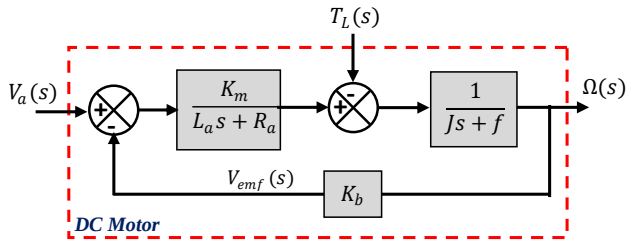

Figure.1 DC Motor model

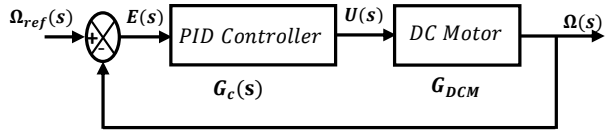

Figure.2 DC motor equivalent circuit with PID controller

the slime mould algorithm (SMA) for efficient PID design.

To tune the PID controller for the aircraft pitch angle control system, zci et al. [8] employed harris hawks optimization (HHO). For PID tuning in an AVR microcontroller, the authors in [9] employed an improved kidney-inspired algorithm(IKIA).

The speed regulation of the DC motor has been the subject of numerous meta-heuristic methods investigations; for example Ekinci et al. [10] employed Henry gas solubility optimization (HGSO) to tune the PID controller for the DC motor speed regulation. Other examples; particle swarm optimization (PSO) [11, 12] which hold a lot of potential for solving a variety of optimization problems, but they have issues with memory capacity and computational load. Jaya optimization algorithm (JOA) [13], gravitational search (GSA) [14], salp swarm algorithm (SSA) [15], atom search optimization algorithm (ASOA) [16] encounters local minima stagnation and a slow rate of convergence, grey wolf optimization (GWO)[17, 18] which was presented as a competitive optimizer for global optimization problems, are heavily influenced by numerous parameters. Similarly like ASO, stochastic fractal search (SFS) [19, 20] has an issue with premature convergence and stagnation and sine — cosine algorithm (SCA) [21]; a recently discovered technique for solving optimization problems.

To achieve the stated goal of higher DC motor performance, a reliable controller is required. Classical PID, on the other hand, as proposed in the literature by various optimization techniques for enhancing performance, may not be capable of getting the optimum results. A fractional-order controller (FOC) can help with this by making it easier to change the control system's time and frequency responses.

Fractional order proportional integral derivative controllers have attracted a lot of attention in academia and industry in recent years [11, 16-17]. Pdlubny [22] et al. introduced the FOC in 1997. The authors conclude in [23] that implementing the FOPID improves performance when compared to traditional ways of adjusting conventional PID controllers. In the case of DC speed control, several fractional order control methods were proposed [16-17, 24-26].

This paper demonstrates the advantages of fractionalized PID based on the HGSO algorithm, which uses fractional order filters to approach integer order transfers in the feedback control loop. By incorporating fractional order integrators into the classical feedback control loop without modifying the overall equivalent closed loop transfer function, the automation designer can apply the properties and dynamics of fractional order to the rational system under consideration.

This paper's contribution to originality can be summarized as follows:

- The main contribution is the first time that the HGSO algorithm based on fractionalized PID controller, HGSO-FPID controller, is used.
- Because these controllers with stated algorithms are the newest ways for determining optimal controller gains, the proposed HGSO-FPID methodology was thoroughly compared to the HGSO-PID [10], ASO-PID [16], GWO-PID [17], PSO-PID [12], IWO-PID [12], SFS-PID [19], and SCA-PID [4].
- Comparative results of transient and frequency responses, as well as load disturbance rejection analyses, conclusively verified the performance and superiority of the recommended fractionalized PID-based HGSO controller over other algorithms.

The rest of this paper is organized as follows. In section 2, the mathematical modeling of DC motor is formulated. In section 3, a brief review of the fundamentals of fractional calculus is presented. Frequency domain analysis of fractionalized integrated is presented in section 4. section 5 describes the HGSO algorithm based on fractionalized PID controller. section 6 presents the simulation results, which are compared to alternative tuning criteria. section 7 concludes with the conclusions.

Table 1. DC motor parameters

Parameter	Value
Armature resistance (R_a)	0.4Ω
Armature inductance (L_a)	$2.7\ H$
motor moment of inertia (J)	$4 \times 10^{-4}\ Kgm^2/s^2$
Coefficient of friction (f)	$0.0022 Nm.s/rad$
Motor torque constant (K_m)	$0.015\ kg\ m/A$
Back EMF constant (K_b)	$0.05\ s$

2. Mathematical model of the DC motor

The purposeful modification of the driving speed to a value required for accomplishing the given work is referred to as DC motor speed control.
Figs. 1 and 2 show, respectively, a DC motor model and its equivalent circuit with a PID controller.

Essentially, a DC motor turns DC electric energy into mechanical energy.

Table 1, displays the DC motor characteristics used in this study/simulation [10, 12, 16-17, 19, 21]:

The following transfer function [10-12] gives the mathematical model for a regulated DC motor (for $T_L = 0$):

$$G_{DCM}(s) = \frac{K_m}{(L_a s + R_a)(Js + f) + K_b K_m} \quad (1)$$

The following open loop transfer function is produced by substituting DC motor parameter values in Eq. (1):

$$G_{DCM}(s) = \frac{\Omega(s)}{V_a(s)} = \frac{15}{1.08s^2 + 6.1s + 1.63} \quad (2)$$

3. Fractional calculus fundamentals

3.1 Definitions

Fractional calculus (FC) is a branch of calculus theory that generalizes a function's integral or derivative to non-integer order $d^n y/dt^n$ n-fold integrals when n is irrational, fractional, or complicated are easier to solve with FC. n is considered fractional in fractional order (FO) systems. The number of applications in which FC has been employed has rapidly increased. These mathematical phenomena allow us to more precisely characterize a real item than traditional integer-order methods. Integration and differentiation are included in the generalized fundamental operator, which is written as:

$$aD_t^{\alpha} = \begin{cases} \dfrac{d^{\alpha}}{dt^{\alpha}} & ,R(\alpha) > 0 \\ 1 & ,R(\alpha) = 0 \\ \displaystyle\int_a^t (d\tau)^{-\alpha} & ,R(\alpha) < 0 \end{cases} \quad (3)$$

Where,

a : Integration Lower limit

t : Integration Upper limit

α : Fractional differentiation or integration Order (The negative sign of α denotes integration while positive sign denotes derivation [27]).

The Grunwald-Letnikov definition is as follows:

$$aD_t^{\alpha} f(t) = \lim_{h \to 0} \frac{1}{h^{\alpha}} \sum_{r=0}^{\frac{(t-a)}{h}} (-1)^r \binom{\alpha}{r} f(t - rh) \quad (4)$$

Where $\omega_r^{(\alpha)} = (-1)^r \binom{\alpha}{r}$ represents the polynomial coefficients of $(1 - z)^{\alpha}$.

The coefficients can also be obtained recursively from

$$\omega_0^{(\alpha)} = 1, \omega_r^{(\alpha)} = \left(1 - \frac{\alpha + 1}{r}\right) \omega_{r-1}^{(\alpha)}, r = 1,2, \ldots \quad (5)$$

The riemann-liouville definition is expressed as:

$$aD_t^{-\alpha} f(t) = \frac{1}{\Gamma(\alpha)} \int_a^t (t - \tau)^{\alpha - 1} f(\tau)\, d\tau \quad (6)$$

Where $0 < \alpha < 1$, h is the step time, and α is the first time occurrence, which is frequently considered to be zero, i.e., $a = 0$. The differentiation is then denoted as $D_t^{-\alpha} f(t)$.
The Caputo's definition is given by

$$0D_t^{-\alpha} y(t) = \frac{1}{\Gamma(1 - \gamma)} \int_a^t \frac{y^{(m+1)}(\tau)^{\alpha - 1}}{(t - \tau)^{\gamma}}\, d\tau \quad (7)$$

The Riemann-Liouville and Grunwald-Letnikov definitions are comparable for a broad class of functions that exist in many engineering applications and real physical systems [28].

3.2 Matsuda's approximation method

Matsuda's method is based on the continuing fraction technique (CFE) [29], which allows for the

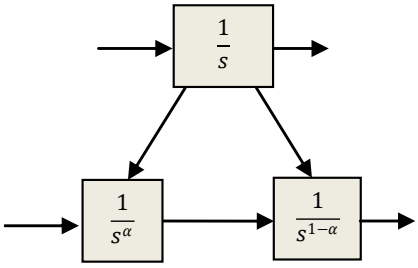

Figure. 3 Integral operator fractionalization

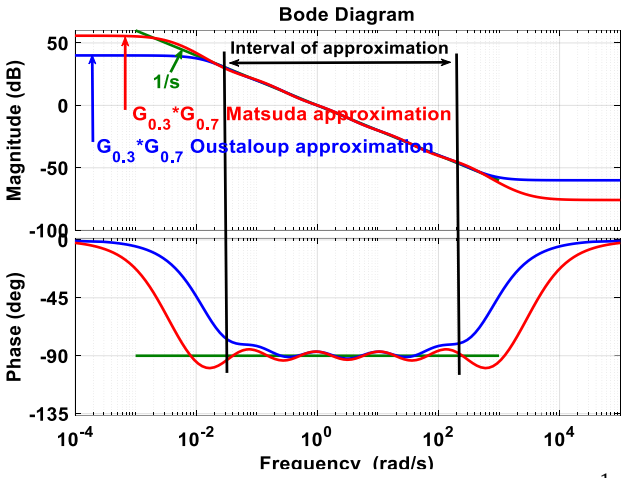

Figure. 4 Bode diagram comparaison of the integration $\frac{1}{s}$ with the oustaloup and matsuda approximations $G_{0.3}(s) \times G_{0.7}(s)$

approximation of an irrational function by a rational one. Assuming that the selected points are s_k , $k = 0,1,2, \ldots N$, the approximation takes on the form:

$$G(s) = \alpha_0 + \frac{s - s_0}{\alpha_1 + \frac{s-s_1}{\alpha_2 + \frac{s-s_2}{\alpha_3 + \cdots}}} \quad (8)$$

Where

$$\alpha_i = v_i(s_i), v_0(s) = G(s), v_{i+1}(s) = \frac{s - s_i}{v_i(s) - \alpha_i}$$

4. Frequency domain analysis of a fractionalized integrator

Let us examine an integrator given by its transform of Laplace:

$$G(s) = \frac{1}{s} \quad (9)$$

The classical integrator fractionalization Eq. (9) as represented in Fig. 3 leads to,

$$\frac{1}{s} = \frac{1}{s^{\alpha}} . \frac{1}{s^{1-\alpha}} \quad (10)$$

Where α is a real number such that $0 < \alpha < 1$.

Using the matsuda approximation approach, as described in section 3.2, and the approximation parameters: $\omega_b = 0.01\, rad/s$, $\omega_h = 1000\, rad/s$, we get the approximated functions $G_{\alpha}(s)$ and $G_{1-\alpha}(s)$ given bellow:

$$G_{\alpha}(s) = G_{0.3}(s) = \frac{0.0803\, s^5 + 94.29\, s^4 + 5357\, s^3 + 24490\, s^2 + 9372\, s + 223.9}{s^5 + 418.6\, s^4 + 10940\, s^3 + 23930\, s^2 + 4212\, s + 35.87} \quad (11)$$

$$G_{1-\alpha}(s) = G_{0.7}(s) = \frac{0.00202\, s^5 + 7.128\, s^4 + 712\, s^3 + 5348\, s^2 + 3363\, s + 141.3}{s^5 + 238.1\, s^4 + 3786\, s^3 + 5040\, s^2 + 504.6\, s + 1.43} \quad (12)$$

Fig. 4 illustrates the frequency domain comparison between the integer order integral operator $1/s$ and the product of the fractional order integral operators approximating filters $1/s^{\alpha}$ and $1/s^{1-\alpha}$ obtained by the Matsuda approximation method.

In Fig. 4, the filter's Bode diagram is placed on the exact responses of 1/s. It can be seen that the matsuda–fujii filter has a larger fitting band. Furthermore, it is clear that this filter product gives a decent approximation of the integral operator in the frequency interval of interest.

5. Fractionalized PID controller based on HGSO algorithm

5.1 HGSO optimization methods

In optimization problems, meta-heuristic methods have found a home. One of the most recent population-based techniques is Henry gas solubility optimization (HGSO). Henry's law of physics influenced this algorithm.

This optimization technique's mathematical modeling can be described in the steps below:

Step1: Initialization

The following equation is used to randomly initialize the search using N gas particles.

$$X_i(t+1) = X_{min} + r \times (X_{max} - X_{min}) \quad (13)$$

In Eq. (13), X_i signifies the position of the ith particle, r denotes an integer produced at random

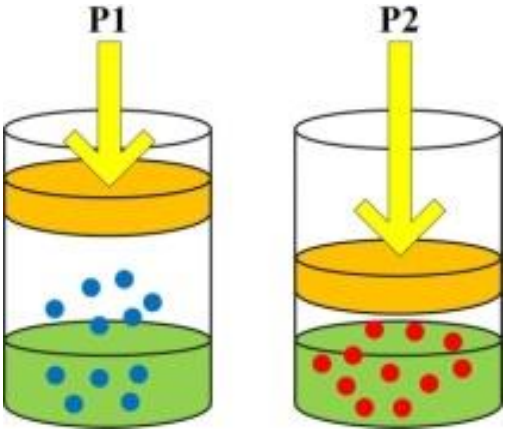

Figure. 5 The Henry gas solubility principle [3]

from the range $[0,1]$, t denotes the number of iterations, and X_{min} defines the lower bound of the search space and X_{max} denotes the upper bound. Henry's constant, partial pressure, and a constant value of each gas particle in the jth cluster are represented by $j(Hj(t))$, $P_{i,j}$, and $j(C_i)$, respectively. Eqs. (14–16) are used to initialize the latter terms, with constant values of I_1, I_2, and I_3 equal to 5.10^{-2}, 100, and 10^{-2}, respectively.

$$H_j(t) = l_1 \times rand(0,1) \quad (14)$$

$$P_{i,j} = l_2 \times rand(0,1) \quad (15)$$

$$C_j = l_3 \times rand(0,1) \quad (16)$$

Step2: Clustering

Because of the many types of gases accessible in HGSO, the population is divided into k groups. Henry's constant, H_j, varies depending on the gas type.

Step3: Fitness evaluation

The considered objective function is performed to analyse the i_{th} gas particle in the j_{th} cluster.

Following the evaluation procedure, the population is ranked based on fitness values. The latter aids in the discovery of the best particle in each cluster ($X_{i,j}$) as well as the total population (X_{best}).

Step 4: Updating coefficient of Henry

Eq. (17) is used to update Henry's coefficient for the j_{th} cluster in each iteration:

$$H_j(t+1) = H_j(t) \times e^{\left(-C_j \times \left(1/T(t) - 1/T^{\theta}\right)\right)} \quad (17)$$

Where:

$$T(t) = e^{(-t/t_m)} \text{ and } T^{\theta} = 298.15$$

Where

t_m and T stand for maximum iterations and tempera -ture values, respectively.

Step 5: Updating Solubility

$S_{i,j}$ is the solubility of the ith gas in cluster j. Eq. (16) is used to change this parameter:

$$S_{i,j} = K \times H_j(t+1) \times P_{i,j}(t) \quad (18)$$

where K is a constant and $P_{i,j}$ is the partial pressure, respectively. These are user-defined values, which are all set to 1.

Step 6: Position Updating

Eq. (19) is used to change the position $X_{i,j}$ in iteration $t+1$:

$$X_{i,j}(t+1) = X_{i,j}(t) + F \times r_1 \times r_2 \times \gamma \times \left(X_{i,best}(t) - X_{i,j}(t)\right) + F \times r_2 \times \alpha \times \left(s_{i,j}(t) \times X_{best}(t) - X_{i,j}(t)\right) \quad (19)$$

Where $\gamma = \times e^{-\left(\frac{F_{best}(t)+\varepsilon}{F_{i,j}(t)+\varepsilon}\right)}$ and $\varepsilon = 0.05$

where r_1 and r_2 are two separate randomly generated values in the range $[0,1]$. The F flag is used to control the search direction, whereas is a user-defined constant with a default value of 1. A search agent's ability to interact with other search agents in its cluster is represented by γ; The impact of other search agents on search agent i is denoted by α. $X_{j,best}$, denotes the best candidate solution in the J_{th} cluster, whereas X_{best} denotes the best solution in the entire population.

Step7: Escaping from Local Optimum

With the help of Eq. (20), the number of worst agents (N_ω) is ranked and chosen:

$$N_\omega = N \times (rand(c_2 - c_1) + c_1) \quad (20)$$

Where $c_1 = 0.1$ and $c_2 = 0.2$.

Step8: Updating worst agents

The following is an updated list of the worst agents:

$$G_{i,j} = G_{min(i,j)} + r \times \left(G_{max(i,j)} - G_{min(i,j)}\right) \quad (21)$$

$G_{i,j}$ is the position of gas i in cluster j, and r is a random number in Eq. (21). The problem's boundaries are G_{min} and G_{max}.

Fig. 5 depicts the principle of Henry gas solubility.

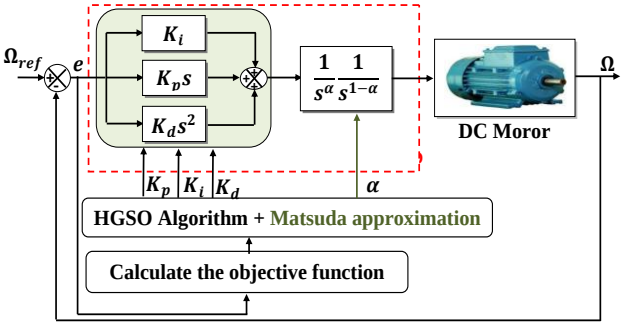

Figure. 6 The proposed HGSO-FPID approach using approximation method for DC speed motor control

Table 2. HGSO-PID parameters for performing optimization problems

Parameter	Value
Total number of gas particles	40
Number of iterations	50
Number of independent runs	20
Lower bound for $[K_p;\ K_i;\ K_d]$	[0.001; 0.001; 0.001]
Upper bound for $[K_p;\ K_i;\ K_d]$	[20; 20; 20]
Dimension for optimization problem	3
Time of simulation (t_{sim})	1s

As can be seen, the volume of the gas in equilibrium drops as the pressure rises.

5.2 Fractionalized PID controller

The proposed fractionalization approach is examined in this study by addressing its application to the transfer function of a feedback control DC motor system given in Eq. (2).

The feedback control loop with a HGSO based on the Fractionalized PID controller is shown in Fig. 6.

In Fig. 6, Ω_{ref} is the reference angular speed, Ω is the output angular speed, (K_p, K_i, K_D) are gains of fractionalized PID and α is the fractional order.

The traditional PID controller to be designed looks like this:

$$G_c(s) = K_p\left(1 + \frac{1}{T_i s} + T_d s\right) \qquad (22)$$

The enhancement The PID control law is adjusted by fractionalizing a control system part, and the operator of integral $1/s$ is fractionalized as expressed in Eq. (10) and illustrated in Fig. 3; that is,

$$\frac{1}{s} = \frac{1}{s^\alpha}\frac{1}{s^{(1-\alpha)}}$$

The fractionalization of the classical PID controller to be created is provided as [30],

$$\begin{aligned} G_c(s) &= K_p(1 + \frac{1}{T_i s} + T_d s) \\ &= \frac{1}{s}\left(\frac{(K_p T_d s^2 + K_p T_i s + K_p}{T_i}\right) \\ &= \frac{1}{s^\alpha}\frac{1}{s^{(1-\alpha)}}\left(\frac{(K_p T_d s^2 + K_p T_i s + K_p}{T_i}\right) \end{aligned} \qquad (23)$$

where, $0 < \alpha < 1$

6. Results of comparative simulations and discussion

The performance of the algorithm in controlling the speed response of a DC motor system given in Eq. (10) is demonstrated in the simulations below. MATLAB/SIMULINK software was used to create the simulations. Table 2 lists the parameters of the proposed HGSO algorithm.

The technique for determining the optimal gains of the PID controller using the HGSO algorithm began with the initialization phase, in which the advanced MATLAB/Simulink model for DC speed control was merged with the HGSO algorithm and approximation method.

The PID controller's gains, which needed to be improved, were assigned to a vector of real numbers that represented each gas particle in the population. The population consisted of N randomly created gas particles and their opposing forces. Then, for each gas particle, a time domain simulation of the DC motor speed control system with the suggested PID controller and unity feedback was performed, and the system's speed response curves were obtained along with the ITAE value given in Eq. (24).

$$J(K_p, K_i, K_d) = \int_0^{t_{sim}} t|e(t)|dt \qquad (24)$$

J refers for performance criteria. It denotes the degree to which the controlled object is similar to the reference model. Where $e(t)$ represents the difference between the set point and the controlled variable, and t is the time.

Fig. 7 depicts a detailed flow chart of the suggested design approach.

For the system model $G_{DCM}(s)$ presented in Eq.

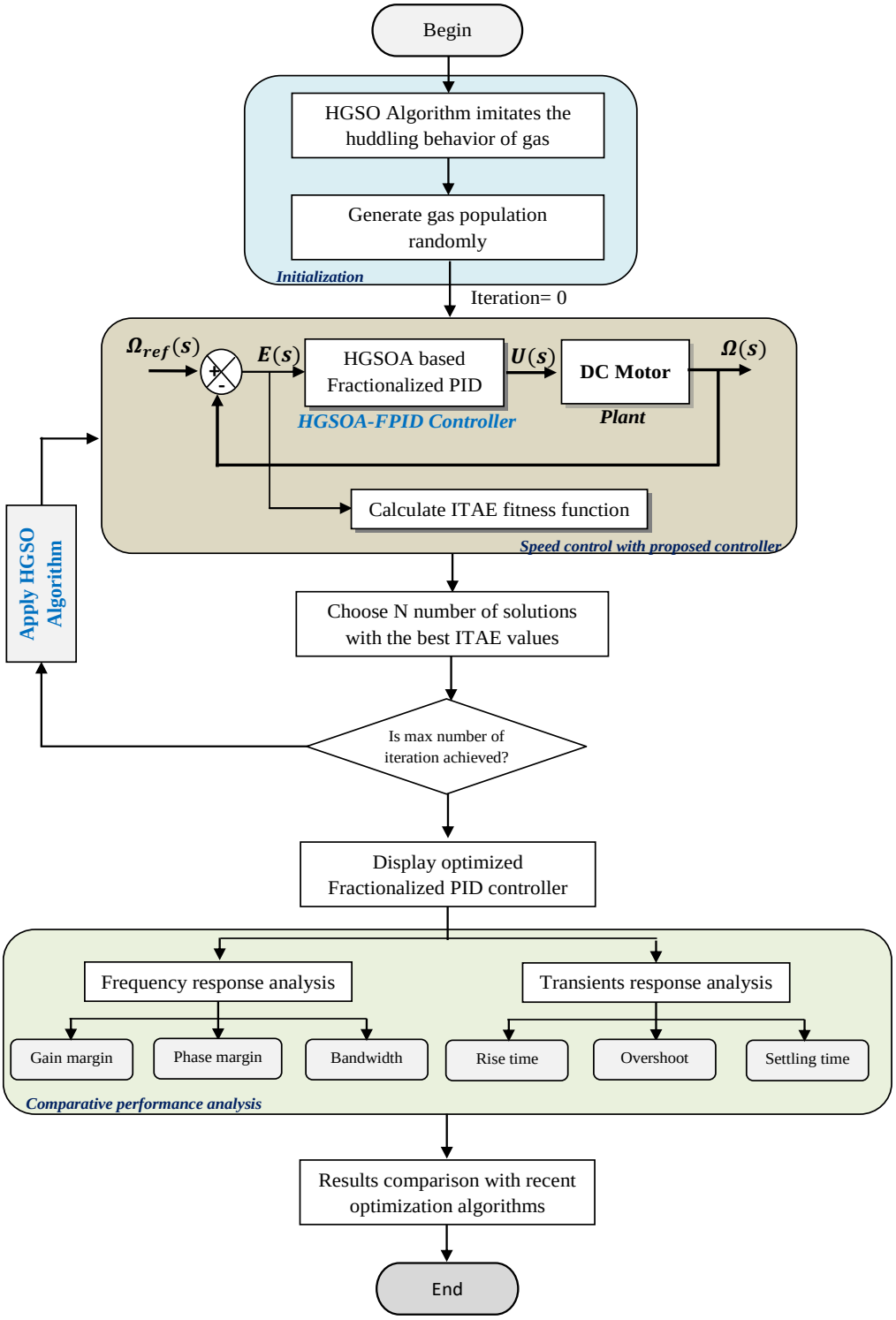

Figure. 7 The proposed design approach for DC speed control is depicted as a flowchart

(2) with the following PID parameters: $K_p = 13.4430$, $K_i = 1.2059$, $K_d = 2.2707$, a PID controller is constructed using the HGSO algorithm. With fractionalized PID and unity feedback, the closed loop transfer function of an DC motor system is:

$$G_{CL_{HGSO-FPID}}(s) = \frac{G_{HGSO-FPID}(s) * G_{DCM}(s)}{1 + G_{HGSO-FPID}(s) * G_{DCM}(s)} \quad (25)$$

As a result, the closed loop transfer function for the HGSO Algorithm with the resulting PID controller has been 'fractionalized,' as shown in Eq.

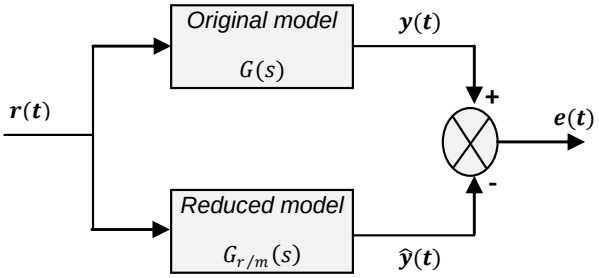

Figure. 8 Error signal for model reduction

(23) with integrator fractional order $\alpha = 0.1$ determined using the Matsuda technique with $\omega_b = 0.01\ rad/s$, $\omega_h = 1000\ rad/s$ and unity feedback is:

$$G_{CL_{FPID-Matsuda}}(s) = \frac{\begin{array}{c}0.002399\ s^{12} + 30.57\ s^{11} + \\ 2.705e04\ s^{10} + \\ 4.308e06\ s^{9} + \\ 1.94e08 s^{8} + 2.828e09\ s^{7} + \\ 1.678e10\ s^{6} + \\ 4.109e10 s^{5} + 3.543e10 s^{4} + \\ 1.086e10\ s^{3} + \\ 1.199e09\ s^{2} + 4.944e07\ s + 5.72e05\end{array}}{\begin{array}{c}1.082\ s^{12} + 849.6\ s^{11} + \\ 1.672e05\ s^{10} + \\ 1.032e07 s^{9} + 2.829e08\ s^{8} + \\ 3.352e09\ s^{7} + 1.807e10\ s^{6} \\ +24.236e10\ s^{5} + 3.593e10\ s^{4} + \\ 1.094e10\ s^{3} + \\ 1.203e09\ s^{2} + 4.948e07 s + 5.72e05\end{array}} \quad (26)$$

The closed loop system with PID based on the HGSO algorithm has a high order. As a result, the entire fractionalized PID controller's memory capacity will be reduced in order to fit better inside the correction loop.

The error signal for model reduction is shown in Fig. 8, where the original model is given by

$$G(s) = \frac{b_1 s^{n-1} + \cdots + b_{n-1}s + b_0}{s^n + a_1 s^{n-1} + \cdots + \alpha_{n-1}s + a_n} \quad (27)$$

Our current goal is to find an approximation integer-order model with a low order, in the form [44]:

$$G_{r/m}(s) = \frac{\beta_1 \mathrm{s}^{\mathrm{r}} + \cdots + \beta_r s + \beta_{r+1}}{\mathrm{s}^{\mathrm{m}} + \alpha_1 s^{m-1} + \cdots + \alpha_{m-1}s + \alpha_m} \quad (28)$$

The following is an objective function for minimizing the H2-norm of the reduction error signal e(t):

$$J = \min_{\theta} \left\| \hat{G}(s) - G_{r/m}(s) \right\|_2 \quad (29)$$

Where θ are the parameters set to be optimized such that:

$$\theta = [\beta_1, \ldots, \beta_r, \alpha_1, \ldots, \alpha_m] \quad (30)$$

Therefore, the closed loop transfer function with the resulting PID controller 'fractionalized' with integrator fractional order $\alpha = 0.1$ approximated using Matsuda method and unity feedback for HGSO Algorithm given in Eq. (26) becomes:

$$G_{CL_{HGSO-FPID}}(s) = \frac{40.32\ s^2 + 238.7\ s + 21.42}{1.08\ s^3 + 46.43\ s^2 + 240.4 s + 21.42} \quad (31)$$

As a result, for different integrator fractional orders $\alpha = 0.2, \alpha = 0.3, \alpha = 0.4$, and $\alpha = 0.5$ applied to DC motor system, the closed loop transfer functions of the HGSO based low order fractionalized PID controller using Matsuda approximation approach are expressed as follows:

- For $\alpha = 0.2$

$$G_{CL_{HGSO-FPID}}(s) = \frac{46.26\ s^2 + 273.9 s + 24.57}{1.08\ s^3 + 52.36\ s^2 + 275.5\ s + 24.57} \quad (32)$$

- For $\alpha = 0.3$

$$G_{CL_{HGSO-FPID}}(s) = \frac{51.07\ s^2 + 302.3\ s + 27.12}{1.08\ s^3 + 57.17 s^2 + 304\ s + 27.13} \quad (33)$$

- For $\alpha = 0.4$

$$G_{CL_{HGSO-FPID}}(s) = \frac{54.15\ s^2 + 320.6 s + 28.76}{1.08\ s^3 + 60.25 s^2 + 322.2\ s + 28.76} \quad (34)$$

- For $\alpha = 0.5$

$$G_{CL_{HGSO-FPID}}(s) = \frac{55.2\ s^2 + 326.8\ s + 29.31}{1.08\ s^3 + 61.3\ s^2 + 328.4\ s + 29.32} \quad (35)$$

6.1 Overshoot, rising time, and settling time comparison

Table 3 lists the PID controller parameters that correspond to the minimal value of the ITAE goal

function for various controllers chosen for fair comparison.

The transfer functions of HGSO/PID, ASOA/PID, GWO/PID, PSO/PID, IWO/PID, SFS/PID and SCA/PID controllers are provided in Eqs. (36-42) using these parameters given in Table 3.

$$G_{CL_{HGSOA-PID}}(s) = \frac{34.06\,s^2 + 201.6\,s + 18.09}{1.08\,s^3 + 40.16\,s^2 + 203.3s + 18.09} \quad (36)$$

$$G_{CL_{ASOA-PID}}(s) = \frac{36.54\,s^2 + 179.2s + 30.78}{1.08\,s^3 + 42.64\,s^2 + 180.8\,s + 30.78} \quad (37)$$

$$G_{CL_{GWO-PID}}(s) = \frac{13.95\,s^2 + 103.5\,s + 8.4}{1.08\,s^3 + 20.05\,s^2 + 105.1\,s + 8.4} \quad (38)$$

$$G_{CL_{PSO-PID}}(s) = \frac{0.24\,s^2 + 22.8\,s + 20.7}{1.08\,s^3 + 6.34\,s^2 + 24.43\,s + 20.7} \quad (39)$$

Table 3. Gain parameters of the proposed controllers and other controllers compared

Controller	K_p	K_i	K_d
HGSOA/PID[10]	13.4430	1.2059	2.2707
ASOA/PID [16]	11.9437	2.0521	2.4358
GWO/PID [17]	6.8984	0.5626	0.9293
PSO/PID [12]	1.5234	1.3801	0.0159
IWO/PID [12]	1.5782	0.4372	0.0481
SFS/PID [19]	1.6315	0.2798	0.2395
SCA/PID [21]	4.5012	0.5260	0.5302

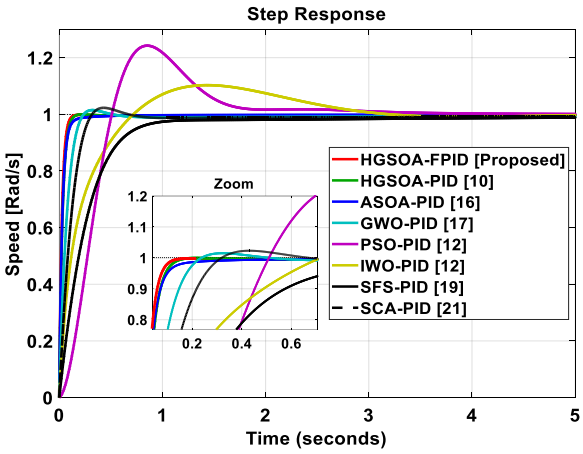

Figure. 9 Comparative speed step responses of DC motor for different controller designs with the proposed HGSOA/FPID controllers for $\alpha = 0.1$

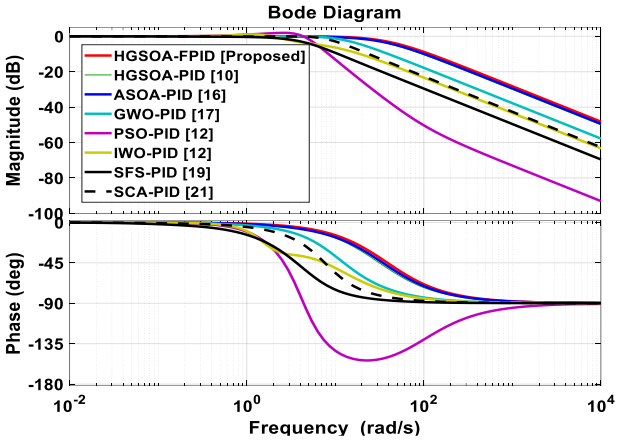

Figure. 10 Comparative bode plots for different controller designs with the proposed HGSOA/FPID controllers for $\alpha = 0.1$

Table 4. Transient response results for $\alpha = 0.1$

Controller type	Overshoot (%)	Settling time (s)	Rise time (s)
HGSOA/FPID [proposed]	**0.00**52	**0.1003**	**0.0579**
HGSOA/PID[10]	**0.0000**	0.1186	0.0684
ASOA/PID [16]	**0.0000**	0.1535	0.0692
GWO/PID [17]	1.4989	0.2052	0.1388
PSO/PID [12]	24.2	1.8	0.356
IWO/PID [12]	6.98	1.25	0.419
SFS/PID [19]	**0.0000**	1.4475	0.5436
SCA/PID [21]	2.3056	0.4899	0.2038

$$G_{CL_{IWO-PID}}(s) = \frac{7.35\,s^2 + 23.7\,s + 29.25}{1.08\,s^3 + 13.45\,s^2 + 25.33\,s + 29.25} \quad (40)$$

$$G_{CL_{SFS-PID}}(s) = \frac{3.592\,s^2 + 24.47\,s + 4.197}{1.08\,s^3 + 9.692\,s^2 + 26.1\,s + 4.197} \quad (41)$$

$$G_{CL_{SCA-PID}}(s) = \frac{7.953\,s^2 + 67.52\,s + 7.89}{1.08\,s^3 + 14.05\,s^2 + 69.15\,s + 7.89} \quad (42)$$

To compare the performances of the proposed approach (HGSO/FPID) for DC speed control system with other existing approaches such as HGSO/PID [10], ASO/PID [16], GWO/PID [17], PSO/PID [12], IWO/PID [12], SFS/PID [19] and SCA/PID [21], a comparative stability analysis was performed in the time and frequency domains; using an input speed

reference of $1rad/s$ are in Figs. 9, 10 where Fig. 9 compares step response to maximum percentage overshoot, rise time (for 10% – 90% tolerance), and settling time (for 2% tolerance) and Fig. 10 compares Bode plot to frequency response performance of gain margin (in decibel), phase margin (in degrees), and bandwidth.

This section looks at one test that represents one order of integration value in a fractionalized PID controller ($\alpha = 1$, in a typical PID controller). Other tests' results are given in a Table 6.

It can be seen in Fig. 10 that, the speed of the DC motor reaches the set point promptly with a negligible overshoot with the proposed HGSO/FPID controller.

Table 4, provides the transient response analysis simulation results (overshoot $[D]$, settling time $[T_s]$, and rise time $[T_r]$) for the integrator fractional order and other controllers obtained by the low order fractionalised PID controller.

The DC speed control system with the suggested HGSO/FPID with Matsuda approximation had the smallest values for both settling and rise times with a negligible overshoot, as shown in Table 4.

Table 5. Comparative frequency response performance analysis results

Controller type	**Gain margin**	**Phase margin**	**Bandwidth**
HGSOA/FPID [proposed]	∞	180	**37.5804**
GSOA/PID[10]	∞	180	31.7975
ASOA/PID [16]	∞	180	32.9113
GWO/PID [17]	∞	180	14.9076
PSO/PID [12]	∞	90.9763	5.5211
IWO/PID [12]	∞	151.1291	3.6993
SFS/PID [19]	∞	180	4.1183
SCA/PID [21]	∞	180	10.1347

Table 6. Transient response results for different integrator order of fractionalized PID

criterions	**HGSOA/FPID controller [Proposed]**			
	$\alpha = 0.2$	$\alpha = 0.3$	$\alpha = 0.4$	$\alpha = 0.5$
Overshoot (%)	0.0431	0.0624	0.0713	0.0738
Settling time(s)	0.0876	0.0795	0.0750	0.0736
Rise time (s)	0.0505	0.0458	0.0432	0.0424

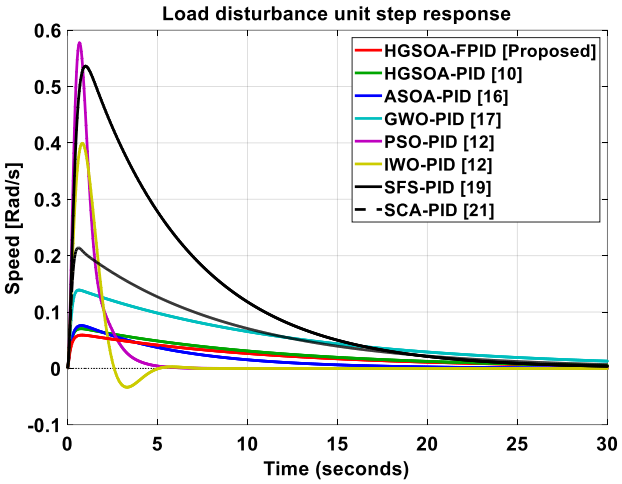

Figure. 11 Comparative study with different approaches based PID and HGSOA/FPID controllers for $\boldsymbol{\alpha = 0.1}$: load disturbance unit step response

In terms of transient stability, fast damping characteristics, and minimum overshoot, the proposed HGSO/FPID controller design approach outperforms not only the HGSOA/PID [10] controller design approach, but also other controller design approaches such as ASOA/PID [16], GWO/PID [17], PSO/PID [12], IWO/PID [12], SFS/PID [19], and SCA/PID [21].

6.2 Comparison of frequency domain analyses

Fig. 10 shows a comparison of Bode graphs with various controller configurations. Table 5, shows the findings of the comparative frequency response performance analysis, including gain margin (in decibels), phase margin (in degrees), and bandwidth (in Hertz).

In terms of frequency response criterion, the table clearly illustrates that the suggested HGSO/PID controller is the most stable system.

Table 6 compares the simulation findings of transient response analysis (overshoot, settling time, and rise time) obtained by the HGSOA/FPID controller for four fractional order integrators $\alpha = 0.2$, $\alpha = 0.3$, $\alpha = 0.4$ and $\alpha = 0.5$ of the fractionalized PID.

In comparison to the state-of-the-art design techniques, the DC speed control system with the suggested HGSO/FPID with Matsuda approximation obtained by changing integrator order of FPID had the shortest values for both settling and rise times with minimum overshoot, as shown in Table 6. (see Table 4).

6.3 Analysis of robustness comparison

A robust controller is necessary to keep the system response within acceptable bounds. As a result, a robustness analysis was performed to determine how stable the proposed system is in the event of a step disturbance.

Fig. 11 compares the proposed HGSOA-FPID controller's disturbance rejection performance to that of the HGSOA/PID [10], ASOA/PID [16], GWO/PID [17], PSO/PID [12], IWO/PID [12], SFS/PID [19], and SCA/PID [21] controller designs for DC speed motor transfer function.

Because it performs a more stable structure, the optimal control strategy for disturbance rejection, as shown in the figure above, is achieved by applying the proposed controller HGSOA/FPID with the Matsuda approximation. Peak errors are high in all of the controllers, but the HGSOA/FPID controller with integrator fractional order $\alpha = 0.1$ performs substantially better.

7. Conclusion

To regulate the DC speed motor system, a fractionalized PID based on the HGSO algorithm was proposed in this study. The HGSO method is used in the controller design process to minimize the ITAE objective function. To demonstrate the superiority and effectiveness of the new proposed HGSO/FPID approach with Matsuda approximation, performance comparisons were made not only with HGSO-based PID controllers but also with various state-of-the-art design approaches such as ASOA/PID [16], GWO/PID [17], PSO/PID [12], IWO/PID [12], SFS/PID [19], and SCA-PID [21]. Time and frequency domain analysis, as well as disturbance rejection analysis, were performed, and the findings reveal that the suggested controller optimizes transient response by minimizing rise time, settling time and overshoot, as well as having strong output disturbance rejection.

As a future work another approximation method for Fractionalized PID controller can be uses and compared the result with the result of this paper also another system can be uses to show the effect of HGSO/FPID controller with different system.

References

[1] R. G. Kanojiya and P. M. Meshram, "Optimal tuning of PI controller for speed control of DC motor drive using particle swarm optimization", In: *Proc. of 2012 International Conference on Advances in Power Conversion and Energy Technologies (APCET), IEEE*, pp. 1-6, 2012.

[2] M. Kushwah and A. Patra, "Tuning PID controller for speed control of DC motor using soft computing techniques-A review", *Advance in Electronic and Electric Engineering*, Vol. 4, pp. 141-148, 2014.

[3] F. A. Hashim, E. H. Houssein, M. S. Mabrouk, W. A. Atabany, and S. Mirjalili, "Henry gas solubility optimization: a novel physics-based algorithm", *Future Generat. Comput. Syst.*, Vol. 101, pp. 646-667, 2019.

[4] F. A. Hashim, E. H. Houssein, K. Hussain, M. S. Mabrouk, and W. A. Atabany, "A modified Henry gas solubility optimization for solving motif discovery problem", *Neural Comput. Appl.*, Vol.32, pp. 10759-10771, 2020.

[5] N. Neggaz, E. H. Houssein, and K. Hussain, "An efficient henry gas solubility optimization for feature selection", *Expert Syst. Appl.*, Vol. 152, pp. 1-22, 2020.

[6] B. S. Yıldız, A. R. Yıldız, N. Pholdee, S. Bureerat, S. M. Sait, and V. Patel, "The Henry gas solubility optimization algorithm for optimum structural design of automobile brake components", *Mater. Test.*, Vol. 62, pp. 261-264, 2020.

[7] D. İzci and S. Ekinci, "Comparative performance analysis of slime mould algorithm for efficient design of proportional–integral–derivative controller", *Electrica*, Vol. 21, pp. 151-159, 2021.

[8] D. Izci, S. Ekinci, A. Demirören, and J. Hedley, "HHO algorithm based PID controller design for aircraft pitch angle control system", *2020 Int. Congr. Human-Computer Interact. Optim. Robot. Appl, IEEE*, pp. 1-6, 2020.

[9] S. Ekinci and B. Hekimoğlu, "Improved kidney-inspired algorithm approach for tuning of PID controller in AVR system", *IEEE Access*, Vol.7, pp. 39935-39947, 2019.

[10] S. Ekinci, B. Hekimoğlu, and D. Izci, "Opposition based Henry gas solubility optimization as a novel algorithm for PID control of DC motor", *Engineering Science and Technology, an International Journal*, Vol. 24, pp. 331-342, 2021.

[11] A. Idir, M. Kidouche, Y. Bensafia, K. Khettab, and S. A. Tadjer, "Speed control of DC motor using PID and FOPID controllers based on differential evolution and PSO", *Int. J. Intell. Eng. Syst.*, Vol. 11, pp. 241–249, 2018, doi: 10.22266/ijies2018.0831.24.

[12] M. Khalilpuor, N. Razmjooy, H. Hosseini, and P. Moallem, "Optimal control of DC motor

using invasive weed optimization (IWO) algorithm", In: *Proc. of Majlesi Conference on Electrical Engineering,Majlesi Town*, Isfahan, Iran, 2011.

[13] R. K. Achanta, and V. K. Pamula, "DC motor speed control using PID controller tuned by jaya optimization algorithm", In: *Proc. of 2017 IEEE Int. Conf. Power, Control. Signals Instrum. Eng.*, pp. 983–987, 2017.

[14] S. Duman, D. Maden, and U. Güvenç, "Determination of the PID controller parameters for speed and position control of DC motor using gravitational search algorithm", In: *Proc. of ELECO 2011 - 7th Int. Conf. Electr. Electron. Eng.*, pp. I-225-I–229, 2011.

[15] B. Hekimog˘lu, S. Ekinci, V. Demiray, R. Dog˘urici, and A. Yıldırım, "Speed Control of DC Motor Using PID Controller Tuned By Salp Swarm Algorithm", In: *Proc. of 2018 Int. Eng. Nat. Sci. Conf. (IENSC 2018)*, pp. 1878–1889, 2018.

[16] B. Hekimog˘lu, "Optimal Tuning of Fractional Order PID Controller for DC Motor Speed Control via Chaotic Atom Search Optimization Algorithm", *IEEE Access*, Vol. 7, pp. 38100–38114, 2019.

[17] J. Agarwal, G. Parmar, R. Gupta, and A. Sikander, "Analysis of grey wolf optimizer based fractional order PID controller in speed control of DC motor", *Microsyst.Technol*. Vol. 24, pp. 4997–5006, 2018.

[18] A. Madadi and M. M. Motlajh, "Optimal control of DC motor using grey wolf optimizer algorithm", *Tech. J. Eng. Appl. Sci.*, Vol. 4, pp. 373–379, 2014.

[19] R. Bhatt, G. Parmar, R. Gupta, and A. Sikander, "Application of stochastic fractal search in approximation and control of LTI systems", *Microsyst. Technol*. Vol. 25, pp. 105–114, 2019.

[20] I. Khanam and G. Parmar, "Application of SFS algorithm in control of DC motor and comparative analysis", In: *Proc. of 4th IEEE Uttar Pradesh Section International Conference on Electrical, Computer and Electronics*, GLA University Mathura, 2017.

[21] J. Agarwal, G. Parmar, and R. Gupta, "Application of sine cosine algorithm in optimal control of DC motor and robustness analysis", *Wulfenia J*., Vol. 24, 2017.

[22] I. Podlubny, L. Dorcak, and I. Kostial, "On fractional derivatives, fractional-order dynamic system and PID-controllers", In: *Proc. of the 36th IEEE CDC*, San Diego, CA, 1999.

[23] Y. Luo et al. "Tuning fractional order proportional integral controllers for fractional order systems", *Journal of Process Control*, Vol. 20, pp.823–831, 2010.

[24] K. Vanchinathan and N. Selvaganesan, "Adaptive fractional order PID controller tuning for brushless DC motor using artificial bee colony algorithm", *Results in Control and Optimization*, Vol. 4, p. 100032, 2021.

[25] R. P. Tripathi, P. Gangwar, and A. K. Singh, "Speed Control of DC Motor with Kalman Filter and Fractional Order PID Controller", In: *Proc. of 2021 International Conference on Advances in Electrical, Computing, Communication and Sustainable Technologies (ICAECT)*, IEEE, pp. 1-4, 2021.

[26] P. Olejnik, P. Adamski, D. Batory, and J. Awrejcewicz, "Adaptive Tracking PID and FOPID Speed Control of an Elastically Attached Load Driven by a DC Motor at Almost Step Disturbance of Loading Torque and Parametric Excitation", *Applied Sciences*, Vol. 11, p. 679, 2021.

[27] J. Sabatier, A. Oustaloup, A. G. Iturricha, and F. Levron, "CRONE control of continuous linear time periodic systems: Application to a testing bench", *ISA Transactions*, Vol. 42, No. 3, pp. 421-436, 2003.

[28] R. Garrappa, "A grunwald–letnikov scheme for fractional operators of havriliak-negami type", *Recent Advances in Applied, Modelling and Simulation*, Vol. 34, pp. 70-76, 2014.

[29] K. Matsuda and H. Fujii, "H∞-optimized wave-absorbing control: Analytical and experimental results", *J. Guidence Control Dyn.*, Vol. 16, No. 6, 1146–1153, 1993.

[30] Y. Bensafia, K. Khettab, and A. Idir, "An Improved Robust Fractionalized PID Controller for a Class of Fractional-Order Systems with Measurement Noise", *International Journal of Intelligent Engineering and Systems*, Vol. 11, No. 2, pp. 200-207, 2018, doi: 10.22266/ijies2018.0430.22.

[31] D. Xue and Y. Q. Chen, "Sub-Optimum H2 rational approximations to fractional-order linear systems", *IDETC/CIE Conf*., California, USA, pp. 01-10, 2005.